

- 1 Swell Wave Progression in the English Channel: Implications for Coastal
- 2 Monitoring
- 3 Thomas Dhoop, Charlie Thompson
- 4 Channel Coastal Observatory, National Oceanography Centre, Southampton, UK.
- 5 Corresponding author: Thomas Dhoop (email: thomas.dhoop@noc.soton.ac.uk)

6 **Abstract**

7 Energetic swell waves, particularly when they coincide with high water levels, can present a significant
8 coastal hazard. To better understand and predict these risks, analysis of the sea levels and waves that
9 generate these events and the resulting coastal impacts is essential. Two energetic swell events,
10 neither of which were predicted by modelled flood forecasts, occurred in quick succession in the
11 English Channel. The first event, on 30th January 2021, produced moderate significant wave heights at
12 or just below the 0.25 year return period along the southwest English coast, but combined with
13 significant swell caused overtopping at East Beach in West Bay and at Chesil Beach. The second event,
14 on 1st February 2021, generated the highest wave energy periods measured at many locations along
15 the southern English coastline and, at High Water, caused waves to run up over the promenades in
16 Poole and Christchurch bays and caused overtopping at Hayling Island. Both events are described in
17 detail and their spatial footprints mapped through joint return period analysis using a copula function.
18 It is found that typical joint return period analysis of water level and significant wave height under-
19 estimates potential impacts, while a joint consideration of water level and wave power describes the
20 31st January event better and a joint consideration of water level and energy period describes the 1st
21 February event best. Therefore, it is recommended that energy period T_e and wave power P are
22 adopted for coastal monitoring purposes and that future studies further explore the use of both
23 parameters for swell monitoring.

24 **Keywords:** Coastal Flooding, Copulas, Joint Return Periods

25 **1. Introduction**

26 Energetic swell waves in the English Channel, particularly when they coincide with high water levels,
27 can present a significant coastal hazard, causing beach erosion and damage to coastal structures and
28 defences (e.g. Draper and Bownas 1983, Sibley and Cox 2014, Palmer *et al.* 2014). Swell is defined as
29 waves that have been generated in another region of the ocean and have propagated out of the area
30 of generation. Typically, the longer-period waves generated by a low pressure system travel faster
31 than the storm and therefore move out of the storm area (Draper and Bownas 1983). Waves that are
32 not generated by local wind conditions may arrive without warning and without wind, therefore taking
33 coastal users and managers by surprise, making swell waves a danger to public safety.

34 From time to time, the UK is subject to long-period swell waves originating from storms developing in
35 the western Atlantic, southeast of Newfoundland. Typically, the energy dissipates over distance.
36 However, in certain cases trapped fetch conditions occur when a depression moves roughly in the
37 same direction and with the same speed as the main wave group, maintaining an input of energy into
38 the longer period waves (Sibley and Cox 2014). The English Channel is a narrow tidal strait adjacent to
39 a large fetch, the Atlantic Ocean, in which trapped fetch conditions can occur (Figure 1). Once swell
40 waves pass through the relatively small window of the Western Approaches, Sibley and Cox (2014)
41 suggest that they are refracted towards the coast by Hurd Deep which lies west to east, in the middle
42 of the English Channel, but are also refracted as they come into shallow water near the coast.

43 This paper uses data from a dense network of wave buoys in the English Channel to describe two swell
44 events that occurred in quick succession in the English Channel. The first on the 30th January and the
45 second on 1st February 2021. Neither event was predicted by modelled flood forecasts, but both
46 caused overtopping of defences along the English south coast, and took coastal engineers and
47 managers by surprise. This analysis will evaluate non-traditional wave parameters as predictors of
48 swell hazard and suggest ways to improve the monitoring of the latter phenomenon with the aim to

49 better support decision making with regards to flood and coastal risk management and further assist
50 modelling and prediction efforts.

51 The wave parameters typically used for the design of coastal structures are significant wave height H_s
52 (in this paper, H_s refers to the spectrally-derived H_{m0}) and the zero up-crossing period T_z . Nonetheless,
53 swell waves have long been appreciated as a contributor to the overtopping of beaches (Carr 1983,
54 Draper and Bownas 1983, Bradbury *et al.* 2007), gravel beach recharge design (Bradbury *et al.* 2011)
55 and the design of defence structures (Hawkes 1999). Indeed, swell conditions are now an integral part
56 of runup and overtopping formulas for beaches (e.g. Poate *et al.* 2016) and a key consideration in the
57 design of coastal defences (EurOtop 2018). Nonetheless, even in recent years, overtopping of
58 defences due to swell events does occasionally occur and has been documented e.g. by Palmer *et al.*
59 2014 and Sibley and Cox 2014. It is important to remember that, although new tools have been
60 developed to assess swell in the design of new assets, many aging assets around England were not
61 designed for extreme long period swell events. Documenting and analysing the metocean conditions,
62 sea levels and waves that continue to cause overtopping of beaches and defences is a useful exercise
63 to better understand the threats presented by swell events and develop methods to better monitor
64 and predict them.

65 The wave parameters typically used for operational beach monitoring are H_s and peak period T_p . In
66 England these parameters are provided in real-time by the National Network of Regional Coastal
67 Monitoring Programmes of England (NNRCMP, 2021), where a “storm alert threshold” is provided for
68 H_s for each wave buoy deployed by the programme as a monitoring tool for coastal engineers and
69 managers (Dhoop & Thompson 2018). T_p values provided on the website are used by some coastal
70 engineers on the south coast of England to monitor for swell waves (pers. comm. Dr S. Cope, Coastal
71 Partners Havant Borough Council). The wave data captured by the NNRCMP is also displayed on the
72 CEFAS WaveNet website (2021) where CEFAS provides a five-day prediction, supplied by the Met
73 Office, for most wave buoys. These data feed into the Met Office wave and tide surge models, and the

74 National Flood Forecasting Service which aims to provide sufficient time for coastal managers to
75 prepare for flooding. The SWEEP Operational Wave and Water Level model is also available on the
76 NNRCMP website (2021). The model was developed by the University of Plymouth Coastal Processes
77 Research Group and provides a three-day forecast of waves, water levels and wave overtopping for
78 the southwest coast of the UK. Both events described in this paper were under predicted by modelled
79 forecasts and although T_p functioned as a good monitoring tool to notify engineers of when the swell
80 arrived at a particular buoy, it did not provide a full appreciation of the energy contained in the swell.

81 In summary, certain swell events continue to prove difficult to predict and monitor. This paper
82 describes the meteorological conditions of two such events and the waves and water levels that they
83 produced. Besides the standard engineering parameters (H_s , T_p , T_z and Direction), two additional
84 parameters are calculated. First, the energy period T_e as an alternative to T_p as it is less subject to
85 rapid changes. As the ratio of the first negative and zeroth moments of the wave spectrum $\left(T_e = \frac{m_{-1}}{m_0}\right)$,
86 the parameter represents more of the lower frequency energy in the spectrum whilst avoiding marked
87 jumps in the time series, typical of T_p . Second, wave power P in an attempt to account for both wave
88 height and wave period in a single parameter. The timing of the swell as it propagated through the
89 Channel and the energy of the swell is then mapped along the English coastline.

90 However, phenomena such as overtopping, beach erosion and coastal flooding are often the result of
91 the combined actions of two or more physical processes, most importantly water level and wave
92 action. Therefore, the wave data is combined with water level data to assess the joint return periods
93 achieved at each wave buoy site. The spatial extent of the swell events is evaluated by mapping the
94 joint return periods of water level and one of three wave parameters: H_s , T_e and P at each wave buoy.

95 This is followed by a description of the overtopping that occurred at East Beach and Chesil on 30th
96 January and at Poole and Christchurch Bays and Hayling Island on 1st February 2021.

97 Finally, recommendations for coastal monitoring and operational beach management purposes are
98 discussed. It is suggested that it would be beneficial to add T_e to the suite of standard wave

99 parameters currently used in coastal monitoring. Realtime provision of both T_p and T_e could provide
100 a more holistic appreciation of a swell event. In addition wave power P , as a measure of both wave
101 height and period, could be a valuable addition for those events where swell is combined with a
102 significant amount of wind-generated waves, although in theory these could be monitored by
103 observing both H_s and T_e .

104 **2. Data and Methods**

105 **2.1. Data Sources**

106 In total, data from 20 wave buoys and seven tide gauges is analysed, allowing for a high-resolution
107 description and analysis of the swell waves and water levels during the 30th January and 1st February
108 events. To accomplish this, three datasets are used.

109 The first and primary dataset is the wave data from the fleet of coastal wave buoys deployed around
110 the English coastline by the National Network of Regional Coastal Monitoring Programmes of England
111 (NNRCMP). The network consists of 37 Datawell Directional Waverider (DWR) MkIII buoys and is
112 funded by the Department for Environment, Food and Rural Affairs (DEFRA) through the Environment
113 Agency. The raw Datawell (2020) 64-bin spectral files and quality-controlled archived data from the
114 18 wave buoys deployed along the English south coast are used (Figure 1). Spectrally-derived and
115 archived parameters are quality controlled according to the procedures published by Mason and
116 Dhoop (2017). The Rye Bay wave buoy is not used as it was (re)deployed on 26th February 2021 and
117 therefore missed both events described in this paper. All buoys used in the analysis are in water depths
118 of approximately 10 m Chart Datum (CD). The longest dataset is Milford-on-Sea (Hampshire) which
119 starts in 1996 and the shortest is Porthleven (Cornwall) which starts in 2011. The mean data length
120 for the wave buoys used is 15 years.

121 The second dataset of wave data is retrieved from CEFAS WaveNet, funded by DEFRA through the
122 Environment Agency. From the 15 wave buoys deployed around the British Isles, the two Datawell
123 DWR MkIII wave buoys deployed in the English Channel at Poole Bay and Hastings are used (Figure 1).

124 Where available, the full 64-bin spectral data is used to derive processed parameters. When not (yet)
125 available, the Iridium telemetry data is used (less than 1% of all wave data used). The Iridium spectra
126 have 27 frequency bins which can vary from spectrum to spectrum as they are calculated to best
127 represent the specific dataset. All post-recovery and telemetry spectra is quality controlled according
128 to the procedures outlined on the CEFAS website (Cefas 2021). The Poole buoy (Dorset) is located in
129 28 m CD water depth and the Hastings buoy (East Sussex) in 43 m water depth CD. The dataset from
130 Hastings spans 19 years, while the dataset from Poole comprises 18 years' worth of measurements.
131 Water levels are retrieved from the UK National Tide Gauge Network, available from the British
132 Oceanography Data Centre (BODC) archive. The network comprises 43 operational tide gauges and is
133 owned by the Environment Agency (EA). The quality-controlled data from the seven tide gauges
134 located along the English south coast are used (Figure 1). The longest record is at Newlyn (Cornwall),
135 which started in 1915 and the shortest at Bournemouth (Dorset) which started in 1996. The mean
136 data length for the tide gauges used is 51 years. Prior to 1993, data frequency was hourly and from
137 January 1993 increased to 15-minutes.

138 **2.2. Wave Power and Energy Period Calculations**

139 Wave power represents the rate of transfer of energy through each metre of wavefront. In this study,
140 wave power is used to account for wave height and wave period, which both have distinct and joint
141 influences on coastal events, in a single parameter. Wave power is defined as (Folley 2016):

$$142 \quad P = \frac{\rho g^2}{64\pi} H_{m0}^2 T_e \quad [1]$$

143 Where ρ is the density of seawater, taken as 1025 kg/m³, g is acceleration by gravity at 9.81 m/s²,
144 H_{m0} ($H_{m0} = 4\sqrt{m_0}$) is the significant wave height based on m_0 , the zero moment of the power
145 spectrum, and T_e the wave energy period.

146 Wave power is proportional to significant wave height squared and the wave energy period. However,
147 most historical and ongoing wave measurement data typically only provide the spectral peak period

148 Tp and mean zero upcrossing period Tz as processed parameters and not the energy period Te needed
149 to calculate wave power. This holds true for the wave data provided by both the NNRCMP and CEFAS
150 WaveNet used in this study.

151 Although Te is not reported as a standard output parameter of a Datawell Directional Waverider MkIII,
152 it can be derived from the raw spectral files from the buoy by calculating the first negative moment
153 and the zeroth moment, where the frequency moment m_n of the spectrum is defined as:

$$154 \quad m_n = \int f^n E(f) df \quad [2]$$

155 Where $E(f)$ is the frequency spectrum (m^2Hz^{-1}), f is the frequency and df is the frequency bandwidth
156 (Hz).

157 The wave energy period Te can then be defined as the ratio of the first negative moment of the
158 spectrum to the zero moment as given by equation 3.

$$159 \quad T_e = \frac{m_{-1}}{m_0} \quad [3]$$

160 Because Te is proportional to the first negative moment of the wave spectrum, the parameter gives
161 more weight to the lower frequencies and therefore the longer periods in the spectrum than wave
162 periods parameters such as Tp or Tz.

163 **2.3. Univariate Extremes Analysis**

164 To gauge the likelihood of the swell events discussed in this study, energy period (Te) return periods
165 are calculated for each wave buoy site. To do this, a peaks-over-threshold approach with the threshold
166 defined as the 99.5th percentile is used, with a 48 hour storm separation window, to create a sample
167 of independent and identically distributed (iid) observations. A generalised Pareto distribution (GPD)
168 is fitted to the sample and parameter estimates are derived using the maximum likelihood method
169 (Coles 2001). Both the threshold and storm separation window are rules-of-thumb to make the
170 analysis more efficient while still providing reasonable parameters for the analysis. The same

171 parameters are used in analyses performed by the NNRCMP and are discussed in detail in Dhoop &
172 Thompson 2018.

173 **2.4. Joint Probability Analysis**

174 The spatial extent of the swell events is examined by producing maps of the spatial footprint of the
175 events based on the joint return period of water level combined with one of three different wave
176 parameters; significant wave height H_s , energy period T_e and wave power P , at each wave buoy.

177 Joint return periods between two time series are calculated using a bivariate copula function. Over
178 the last fifteen or so years, copula functions have been widely used in coastal engineering to examine
179 a combination of wave heights and periods (De Waal and Van Gelder 2005), storm surges and wind
180 waves (Bernadino et al. 2013; Wahl et al. 2012) and sea level and wave height (Mazas and Hamm
181 2017). It should be noted that, as mentioned above, this study uses a number of heuristics to make
182 the analysis easier to apply to all wave buoy sites while providing the most reasonable spatial footprint
183 and does not attempt to provide any design characteristics for any particular location.

184 The following four-step methodology is implemented in MATLAB and is typical to UK coastal
185 engineering as the same steps are used in the JOIN-SEA software (Hawkes et al 2002):

- 186 a. Data selection of the joint time series
- 187 b. Modelling of the marginal distributions
- 188 c. Analysis of the dependence structure
- 189 d. Estimation of joint return periods

190

191 **2.4.1. Data Selection of the Joint Time Series**

192 Samples for dependence modelling were extracted from concurrent time series of water levels and
193 wave parameters using a multivariate threshold similar to Li et al. (2014). It is assumed that, in order
194 for high and/or energetic swell waves to cause significant beach erosion, overtopping or coastal

195 flooding at all wave buoy sites, they must occur at or around a high water level. Therefore, first a
196 subsample of the 5% highest tides and their concurrent wave parameters is extracted. From this
197 subsample, the sample for dependence modelling is extracted by applying a high threshold for the
198 wave parameter (Figure 2). This threshold varies site by site and is determined by the desired sample
199 size. It can be argued a sufficiently large sample is needed to capture dependence between variables.
200 Therefore, we follow Mazas and Hamm (2017), and strive for 20 events per year (i.e. the shortest time
201 series of 10 years has a desired sample size of 200 events).

202 Independent events are assured by applying a storm separation window of 48 hours. This window was
203 adopted as a rule of thumb for all sites as a compromise between assuring independent observations
204 and losing valid observations due to tightly clustered, but independent storms (e.g. the unusual 2013-
205 2014 storm season, see Malagon Santos et al. 2017).

206 **2.4.2. Marginal Distributions**

207 The joint probability approach taken in this study uses a mixture distribution: an extreme value
208 analysis is carried out for modelling the tail of the distributions of water level and the wave parameter,
209 while the dependence (Section 2.4.3) is modelled from the sample of joint high water levels and the
210 wave parameter derived in section 2.4.1.

211 Similar to the univariate extremes analysis described in section 2.3, for water level and each wave
212 parameter, a threshold is set above which the exceedances are modelled by a GPD. The value of the
213 threshold is again determined by the desired sample size. Following Bernardara et al (2014) and Mazas
214 and Hamm (2017), 10 events per year are strived for (i.e. e shortest time series of 10 years has a
215 desired sample size of 100 events). Independence is again assured by applying a storm separation
216 window of 48 hours.

217

218

219 **2.4.3. Dependence Structure**

220 Dependence between water level and the wave parameter is measured using Kendall's rank
221 correlation coefficient τ , a well-known nonparametric measure of dependence (e.g. Wahl et al 2012).

222 Following Sklar's theorem (1959), the joint cumulative distribution function $H_{X,Y} = \mathbb{P}[X \leq x, Y \leq y]$
223 can be described by the univariate marginal distributions of X and Y , F_X and F_Y , via a copula C :

224 $H_{X,Y}(x, y) = C(F_X(x), F_Y(y))$ [4]

225 The copula function used in this study needs to be applicable to a large number of wave buoy sites
226 with different wave climates and with potentially different levels of dependence between water level
227 and the wave parameter. Because the calculated joint return periods need to be comparable to one
228 another, a bivariate normal copula, or Gauss copula was used for all sites (as is used in the JOIN-SEA
229 software, Hawkes et al. 2002). The Gauss copula is described by the dependence parameter θ (or
230 correlation parameter) which is derived using the copulaparam function in MATLAB.

231 **2.4.4. Estimation of Joint Return Periods**

232 Joint return periods for each swell event are evaluated by plotting two peaks on a joint return period
233 plot; (a) the peak of the wave parameter with the associated water level and (2) the highest water
234 level during the event with its associated wave parameter (Figure 3). The plot is constructed by
235 extracting the contours from the copula at nine intervals (2, 5, 10, 15, 20, 25, 50, 75 and 100 years
236 joint return periods), shaped by the dependence parameter θ , while the marginal distributions
237 calculated in section 2.4.2 inform the x and y axes. The highest joint return period achieved between
238 the two peaks is considered the joint return period of the event.

239 The concept of return periods can be ambiguous, particularly in a bivariate context. Despite work by
240 Serinaldi (2015) outlining the misinterpretations of return periods in a multivariate setting, return
241 periods are still a staple when discussing probabilities in coastal engineering and are therefore still
242 used in this study. For the sake of clarity, because the sampling strategy described in section 2.4.1

243 extracted exceedances of both water level and a wave parameter, the joint return periods in this work
244 are to be understood as the return periods associated with the joint exceedances of both variables.

245 **3. Results**

246 **3.1. 30th January 2021**

247 **3.1.1. Swell Generating Mechanism**

248 To find the generating area for the swell measured on 30th January 2021, the UK Met Office synoptic
249 analysis charts for the previous few days were examined. The chart for 12:00 UTC on 28th January 2021
250 shows a new depression southeast of Newfoundland (low 973 mb) (Figure 4, Table 1). This low quickly
251 moved in a northeast direction and by 00:00 UTC, on 29th January it can be seen as a low that had
252 deepened to 967 mb. Twelve hours later, the depression had continued its northeasterly movement
253 at a slightly slower pace and persisted as a low at 968 mb. At this point, the westerly winds generating
254 waves on its southern flank are conservatively estimated from the synoptic chart by the authors to be
255 around 55-60 knots. Such wind speeds are not uncommon in an Atlantic storm. The low continued its
256 northeasterly movement filling to 975 mb by 00:00 UTC on 30th January. Twelve hours later, the low
257 was positioned west of Land's End and had filled to 981 mb. Finally, by 00:00 UTC on 31st January the
258 remains of the depression centred over Nantes, in France.

259 **3.1.2. Swell Propagation Through the Channel**

260 To track the swell waves as they travelled through the English Channel, their first manifestation in
261 peak period T_p is plotted on a timeline (x-axis on Figure 5). The first instances of T_p were site specific
262 and in the range of 15.4s to 22.2s. The energy contained in the swell manifested at each wave buoy
263 site is shown as the peak energy period that was achieved at the site during the event (y-axis on Figure
264 5). To investigate how common the swell measured at each wave buoy location is and to make the
265 swell comparable between sites, the T_e return period achieved at each site is calculated (circle size on
266 Figure 5).

267 On 30th January, the swell first manifested at Porthleven at 14:00 UTC. Between 15:00 UTC and 15:30
268 UTC, the waves had reached Looe Bay and western Lyme Bay. By 16:30 UTC, West Bay and Chesil
269 recorded the swell also. By 18:00 UTC the swell manifested in the Christchurch and Poole Bays. One
270 hour later, the waves had refracted around the Isle of White and reached Hayling Island. The most
271 easterly location where swell was visible in Tp was Seaford at 20:30 UTC. From its first measurement
272 at Porthleven to the eastern most measurement at Beachy Head, the swell travelled about 430
273 kilometres in about 6.5 hours, moving at an average speed of 66 km/h or 36 knots. The highest return
274 periods were achieved at the Looe Bay, West Bay and Chesil wave buoys.

275 Figure 5 shows that, at some buoys, the swell waves manifested in Tp later than one would expect
276 based on their location and the timing of their detection at neighbouring buoys. This is the case at
277 Penzance, Dawlish and Pevensey Bay. The primary reason for this is the prevalence of locally-
278 generated wind waves in the spectra of those sites, hiding the swell component until the swell
279 manifested strongly enough in the spectrum. A secondary reason may be that the buoys are all east-
280 facing and it may therefore take some time for the swell to refract around to reach them.

281 **3.1.3. Spatial Footprint**

282 The spatial footprint of this event is mapped by calculating a number of joint return periods at each
283 wave buoy site using a copula function, focusing on the time of primary concern when they occur at
284 or around High Water. Joint return periods are calculated for water level and one of three wave
285 parameters: significant wave height H_s , Energy period T_e and wave power P .

286 Because the swell passed through the channel around High Water, the high water levels pushed the
287 joint return periods above 1 in 2 years at all sites where the swell was observed (Figure 6). Looking
288 closer at the joint water level and significant wave height H_s footprint, higher joint return periods were
289 achieved between Porthleven in Cornwall and Tor Bay in West Lyme Bay (numbers 2 and 5 on Figure
290 1) with joint water levels and wave heights at Penzance, Looe Bay, Start Bay and Tor Bay (numbers 1,
291 3, 4 and 5 on Figure 1) exceeding the 1 in 5 year joint return period.

292 Investigating the joint water levels and energy periods T_e achieved at the buoys, a 1 in 5 year joint
293 return period was achieved at almost all instruments where the swell was measured, ranging from
294 Porthleven in Cornwall to Seaford in East Sussex (numbers 2 and 17 on Figure 1).

295 Finally, examining the map of joint water level and wave power, the latter itself being a function of
296 energy period T_e and significant wave height H_s squared, high joint return periods were achieved at
297 Porthleven (1 in 25 years) and Looe Bay (1 in 20 years) (numbers 2 and 3 on Figure 1). 1 in 5 year joint
298 return periods were also exceeded at Start Bay, West Bay and Chesil (numbers 4, 7 and 8 on Figure 1).
299 Further east, in the Christchurch and Poole Bays, the 1 in 5 year joint return period was exceeded at
300 Poole Bay (number 11 on Figure 1), but not at the two buoys located closer inshore.

301 **3.1.4. Impact at East Beach and Chesil**

302 At East Beach in West Bay, small scale overtopping occurred during the 30th January swell event. The
303 event came as a surprise and caused significant erosion, resulting in some ‘cliffing’ of the beach (Figure
304 7). However, it should also be noted that the crest width of the beach was already much reduced
305 before the event. The ‘cliffing’ is believed to have been caused by the high content of fine material
306 present in the shingle at the time. This was likely disturbed during the construction of a new rock
307 revetment in 2019. Prior to this, the clean shingle had no cohesive properties. With time, it is expected
308 the fine material will wash from the single (pers. comm. Martin Worley, Environment Agency).

309 Chesil Beach suffered notable overtopping with flooding around Chiswell and Brandy Row. Several
310 cars were damaged and a significant amount of shingle was swept onto the promenade and street.
311 The lower beach foreshore suffered from erosion whilst the upper beach experienced accretion, with
312 material deposited just below the crest of the open beach and level with the top of the sea wall at
313 Chesil Cove. It is possible this exacerbated the overtopping in places by providing a shingle ramp for
314 wave runup, allowing water to overtop the sea wall (Dave Picksley, Environment Agency). The erosion
315 at Chiswell can clearly be seen on the two photos taken before and after the event as part of the
316 Southwest Regional Coastal Monitoring Programme’s CoastSnap project (Figure 8).

317 **3.2.1st February 2021**

318 **3.2.1. Swell Generating Mechanism**

319 To find the generating area for the swell measured on 1st February 2021, the UK Met Office synoptic
320 analysis charts for the previous few days were again consulted. The chart for 00:00 UTC on 30th January
321 2021 shows a new depression southeast of Newfoundland (low 957 mb) (Figure 9, Table 2). This low
322 moved in a northeast direction and by 12:00 UTC, on 30th January, it can be seen as a low that had
323 filled to 962mb. Twelve hours later, the depression had continued its northeasterly movement at a
324 slightly more rapid pace and continued to fill at 969 mb. At this point, the westerly winds on its
325 southern flank are conservatively estimated from the synoptic chart by the authors to be around 55
326 knots, similar to the 30th January event and not uncommon for an Atlantic storm. The low continued
327 its northeasterly movement filling to 978 mb by 12:00 UTC on 31st January. By 00:00 UTC on 1st
328 February the depression had weakened and lost its identity, and was incorporated in a complex low
329 pressure system, having filled to 987 mb. The final remains of the depression appear to be centred
330 between Bremen and Dortmund, in Germany.

331 **3.2.2. Swell Propagation Through the Channel**

332 The first manifestation of the waves in peak period T_p (values were site-specific and ranged between
333 18.2s and 25s) is plotted against swell intensity (peak energy of the event), and T_e return period
334 (Figure 10).

335 On 1st February, the swell was first measured by the Porthleven buoy at 03:30 UTC and reached Looe
336 Bay by 05:30 UTC. West Bay and Chesil were confronted with the swell around 06:30 UTC. By 07:30
337 UTC, the waves reached the Poole and Christchurch Bays. One hour later, the swell had refracted
338 around the Isle of Wight and reached Hayling Island. At 11:30 UTC the swell reached Seaford at Beachy
339 Head and by 12:00 UTC, the waves arrived at Folkestone which is the eastern most located wave buoy
340 where the swell manifested in T_p . From their first measurement at Porthleven to the eastern most
341 buoy where the swell manifested in T_p in Folkestone, the swell waves travelled about 510 kilometres

342 in about 8.5 hours, travelling at an average speed of 60 km/h or 32 knots. The highest return periods
343 were achieved at Boscombe, Poole Bay and Hayling Island.

344 Figure 10 shows that again, at some buoys, the swell waves manifested in T_p later than one would
345 expect based on their location and when the neighbouring buoys registered the swell. This is the case
346 at Penzance, Start Bay, Tor Bay, Dawlish, Chesil, Sandown Bay, Pevensey Bay and Hastings. A possible
347 explanation is that the majority of these are east-facing sites where it would take some time for the
348 swell to refract around to reach the particular wave buoy.

349 **3.2.3. Spatial Footprint**

350 Because waves are the most dangerous during high water levels, at each wave buoy, the joint return
351 period of water level and one of three wave parameters is calculated: significant wave height H_s ,
352 energy period T_e and wave power P .

353 As was the case during the 30th January event, because the swell passed through the channel around
354 High Water at most wave buoy sites, the 1 in 2 year joint return period was exceeded at all locations
355 (Figure 11). Examining the joint water level and significant wave height footprint, at no location was
356 the 1 in 2 year joint return period exceeded, making it clear that wave heights did not contribute in
357 any significant way to the event. The same pattern holds true for the joint return periods of water
358 level and wave power; at no location was the 1 in 2 year return period exceeded.

359 In contrast, looking at the map showing joint water level and energy period T_e , the 1 in 2 year return
360 period was exceeded at all sites with the exception of Tor Bay (number 5 on Figure 1) on the southeast
361 coast of Devon. At all other sites, at least the 1 in 5 year return period was exceeded with the 1 in 100
362 year return period exceeded at Boscombe in Poole Bay and at Hayling Island in the Solent (numbers
363 10 and 14 on Figure 1).

364

365

366 **3.2.4. Impact at Christchurch and Poole Bay and Hayling Island**

367 At Hayling Island, significant and dangerous overtopping occurred during the 1st February 2021 swell
368 event. This was unexpected and caused flooding in the gardens along Southwood Road, although the
369 flood defences managed to retain the majority of the overtopping within the promenade. In places,
370 the waves flattened the crest of the beach which required emergency repairs and deployment of plant
371 to reinstate the standard of protection (pers. comm. Dr A. Pearce, Coastal Partner Havant Borough
372 Council) (Figures 12 & 13).

373 The 1st February swell event also caused a surprising amount of water to run up over the promenades
374 in Poole and Christchurch Bays which likely cannot be just attributed to antecedent beach levels (pers.
375 comm. Dr M. Wadey, Bournemouth, Christchurch and Poole (BCP) Council).

376 It is also worth mentioning that on 26th February 2021, part of the east wing of Hurst Castle, located
377 on the Hurst Spit shingle bank, collapsed. Although the collapse is not a direct result of the two swell
378 events described in this study – the foundations of the east wing were already severely undermined –
379 the two swell events may have expedited the collapse.

380 **4. Discussion**

381 **4.1. 30th January 2021**

382 The reported significant impacts of the 30th January event are focused along the coastline of western
383 Dorset. At East Beach in West Bay small scale overtopping and erosion occurred resulting in the
384 ‘cliffing’ of the beach, although it should be noted that the beach was already depleted. Also at Chesil
385 Beach notable overtopping occurred, damaging cars and moving significant amounts of shingle from
386 the lower foreshore to the upper beach, onto the promenade and into the street.

387 The storm that generated the swell originated on 28th January as a new Atlantic depression southeast
388 of Newfoundland which tracked due east, with forcing winds moving in a relatively straight line
389 relative to the curvature of the earth which directed long-period swell waves directly towards the UK.

390 During the strongest storm development period, when the low was travelling across the Atlantic,
391 trapped fetch conditions as described by Sibley and Cox (2014) may have occurred as the centre
392 travelled at a speed between 28 and 36 knots with a gradient wind speed on the southern flank
393 estimated at around 55-60 knots (Table 1), suggesting that the speed of movement of the low centre
394 kept track with the group wave speed. However, the centre did not enter the English Channel, as
395 around midday on 30th January, the storm changed direction bending south past Land's End towards
396 Brittany in France.

397 When the swell first arrived at West Bay and Chesil between 16:30 UTC and 17:00 UTC, a surge of
398 ~27.9cm was measured at the Weymouth NTSLF tide gauge. At the peak of the event, defined as when
399 significant wave height H_s peaked at 3.49m at West Bay and 4.04m at Chesil, between 20:30 UTC and
400 21:30 UTC, the surge had dropped to ~14.65 cm. High Water occurred close to the peak at 20:00 UTC
401 with a maximum water level of 1.32m OD on a spring tide. At West Bay, Peak period T_p peaked at 20s,
402 energy period T_e at 15s, wave power P at 86 kW/m² and peak wave direction was 210 degrees
403 (southwest by south). At Chesil, T_p peaked at 22.2s, T_e at 12.1s, P at 120 kW/m² and peak wave
404 direction was 220 degrees (southwest).

405 The 30th January event was driven by a combination of swell entering the English Channel and low
406 pressure centred west of Land's End generating high wave heights for the southwest regions of the
407 English coastline. These conditions resulted in high wave powers generated at the Porthleven and
408 Looe Bay wave buoys, exceeding the 1 in 20 and 1 in 15 years joint return periods for water level and
409 wave power, respectively. Due to the nature of the event, the spatial footprint that captured the
410 impact of the event best is the combined consideration of water level and wave power.

411 Two observations regarding the impact of wave heights during the event are worth pointing out. First,
412 neither at West Bay nor Chesil, the two sites where overtopping was recorded, did significant wave
413 height H_s exceed the storm alert threshold on the NNRCMP website, emphasizing again the well-
414 established point that energetic long period waves are an important component of overtopping and

415 beach erosion and are therefore important to monitor. Nonetheless, the second observation is that
416 no overtopping was reported at either site during the even more energetic 1st February event, likely
417 because significant wave heights were quite low (section 4.2.1). Other factors that likely influenced
418 the different impacts of both swell events at West Bay and Chesil are the storm tracks and wave
419 directions, but detailed analysis of these are outside the scope of this paper.

420 A final observation worth considering is that, when monitoring swell by tracking peak period T_p , the
421 wind waves generated by the depression off Land's End managed to hide the swell in this parameter
422 for a considerable amount of time at locations like Penzance and Dawlish before the swell peak
423 became dominant in the wave spectrum.

424 **4.2.1st February 2021**

425 The reported impacts of the 1st February event are centred on the coastline of east Dorset and the
426 Solent in Hampshire. At the Poole and Christchurch Bays, water ran up over the promenades and at
427 Hayling Island, a significant amount of overtopping occurred, flattening the crest of the beach and
428 requiring emergency repairs and deployment of plant on the beach.

429 The storm that generated the swell originated on 30th January as a new Atlantic depression southeast
430 of Newfoundland. Also this storm tracked northeast with forcing winds travelling in a relatively
431 straight line pushing long-period swell waves directly towards the British Isles. Again, trapped fetch
432 conditions may have occurred as the storm crossed the Atlantic with the centre travelling at speeds
433 between 33 and 39 knots with a gradient wind speed on the southern flank estimated at around 55-
434 60 knots, suggesting the movement of the low kept track with the group wave speed. However, by 1st
435 February, the depression had weakened and became incorporated in a complex low pressure system
436 that moved across the English Channel, potentially continuing to feed the wave group passing through.
437 When the swell waves arrived at the buoys deployed in Poole Bay and at Hayling Island, at 07:30 UTC
438 and 08:30 UTC respectively, a surge of ~ 32.7 cm was measured at the Portsmouth NTSLF tide gauge.

439 At the peak of the event, defined as when energy period T_e peaked at 18.7s at Boscombe and 20.6s
440 at Hayling Island, between 12:30 UTC and 13:30 UTC, the surge dropped slightly to 27.1cm. High Water
441 occurred one hour after the peak of the event at Boscombe and during the peak at Hayling Island with
442 a maximum water level of 2.16m OD on a spring tide. At Boscombe, significant wave height H_s peaked
443 at 1.42m, peak period T_p at 25s, wave power P at 11 kW/m² and peak wave direction was 186 degrees
444 (south by west). At Hayling Island, H_s peaked at 1.92m, T_p at 25s, P at 29 kW/m² and peak wave
445 direction was 180 degrees (south).

446 The 1st February event and its related impacts were entirely driven by the swell waves travelling
447 through the Channel. The complex low travelling across the channel did not generate any significant
448 wind speeds or wind waves. These conditions resulted in a calm weather day during which an
449 exceptionally energetic swell passed through the channel, generating some of the highest energy
450 period measurements on record at the buoys in the channel, but relatively low significant wave height
451 measurements. Due to these conditions, the spatial footprint that captured the impact of this event
452 best is the combined consideration of water level and energy period T_e .

453 The 1st February event is close to a schoolbook example of the dangers swell events pose, especially
454 during a calm day. At the Poole and Christchurch Bays, waves unexpectedly running up the
455 promenades are a danger to the public, while at Hayling Island the swell significantly flattened the
456 beach crest. Furthermore, the swell entered at an angle in the channel, and was energetic enough, to
457 travel all the way through, still being distinctly visible in the data from the Folkestone buoy in Kent.

458 **4.3. Implications for Coastal Monitoring**

459 The two consecutive but quite different swell events documented in this paper present an opportunity
460 for coastal monitoring programmes to reflect on how waves, and in particular swell waves, are
461 measured and reported.

462 Currently, long-period swell monitored through measurements is primarily done by observing (or
463 setting an alert for) peak period T_p . Because T_p is defined by the period at the wave spectrum peak it
464 is subject to rapid changes. Moreover, if there are more than two distinct frequency components of
465 similar peak energy, the time series of T_p can appear to fluctuate markedly. These properties of the
466 parameter can be advantageous and will typically result in swell being first picked up in this parameter.
467 However, as was the case at some locations during the 30th January event, swell can also remain
468 hidden in T_p if sufficient wind waves are generated for the wind wave peak on the spectrum to
469 dominate the swell peak. A solution to this is to partition the wave spectrum into its wind and swell
470 components and focus on the peak period for the swell component only, thereby excluding any
471 contamination of wind-wave energy. However, because the lower frequencies in a standard (Datawell)
472 wave spectrum are not as finely-resolved, relatively large step-changes in a time series of T_p swell will
473 remain. Such a bimodal wave spectrum is typically referred to as a bimodal sea state and is monitored
474 post hoc by the NNRCMP by calculating the occurrence of bimodal seas as a monthly percentage
475 (Mason & Dhoop 2018) and is available as a regularly updated spreadsheet (NNRCMP 2021).

476 A well-established tool for wave monitoring is the definition of a threshold condition, such as the
477 storm alert threshold defined on the real-time data pages of the NNRCMP website. A similar threshold
478 condition could prove useful for swell monitoring. However, the rapidly-changing nature of T_p makes
479 this parameter unsuitable for such use. In an attempt to quantify the energy contained in the swell
480 events discussed in this paper, the energy period T_e is found to provide a much smoother time series.
481 As the ratio of the first negative and zero moments of the wave spectrum, the parameter represents
482 more of the lower frequency energy in the spectrum whilst avoiding marked jumps in the time series.
483 Figure 14 shows a time series of peak period T_p and energy period T_e as measured by the wave buoys
484 at West Bay, Chesil, Boscombe and Hayling Island covering both swell events discussed above. In red,
485 a horizontal line was added as an indicative 'swell alert threshold' at the 0.25 year return period for
486 energy period. The threshold was chosen to mimic the 0.25 years return period threshold used for

487 significant wave height H_s by the NNRCMP. The reasoning being that, on average, four times per year
488 conditions occur which have the potential to move a significant quantity of beach material. The
489 threshold condition applied in Figure 14 appears to function relatively well; the threshold is exceeded
490 at West Bay and Chesil during both events, while at Boscombe and Hayling Island the threshold is
491 exceeded only during the 1st February event, matching the findings in this paper.

492 As Mason *et al.* (2008) had suggested before, the addition of energy period T_e to the current set of
493 wave parameters provided as an industry standard in coastal monitoring could prove beneficial to
494 monitoring swell in the future. An additional benefit of T_e is that it is the standard wave period used
495 for wave run-up and overtopping formulae (van de Meer 2008) and may therefore be of particular use
496 to calibrate and provide a check on overtopping models. A complication to this end is that T_e is
497 typically not a standard output of most wave measuring instrumentation. Nonetheless, it can be
498 derived from the wave spectrum, a dataset already provided by most providers of wave data (e.g.
499 CEFAS, NNRCMP) in England, in a straightforward manner. Alternatively, the parameter can be derived
500 from additional instrument specific parameters (for an example using Datawell DWR MkIII parameter
501 outputs, see Appendix 1).

502 It is also worth noting that, despite the irregularities noted in sections 3.1.2 and 3.2.2, swell propagates
503 through the English Channel from west to east in a progressive manner. Up to a point, it is therefore
504 possible to receive a couple of hours early warning of incoming swell at those locations further east
505 up the Channel by monitoring T_p and T_e at more westerly located wave buoys. Furthermore, by
506 partitioning the wave spectrum in its wind and swell components and by monitoring the peak period
507 of the swell component only, it is possible to avoid swell remaining hidden due to a wind-wave peak
508 dominating the spectrum. A closer examination of the time dependencies between T_p , T_p swell and
509 T_e at different locations along the southern English coastline could prove useful for coastal monitoring
510 purposes.

511 Finally, while it is perfectly reasonable to be well-informed about both swell events by monitoring H_s
512 in tandem with energy period T_e , once the latter is provided as a parameter for monitoring purposes,
513 it is a relatively small effort to also provide wave power as a parameter that incorporates both wave
514 height and period. Wave power P is particularly useful when a swell event is combined with locally
515 generated waves such as the 30th January event.

516 **5. Conclusions**

517 Energetic swell waves, particularly when they coincide with high water levels, can present a significant
518 coastal hazard. Two such events occurred in quick succession in the English Channel. The first, on 30th
519 January 2021, was driven by a combination of swell entering the English Channel and a depression
520 centred west of Land's End generating moderate wave heights for the southwest regions of the English
521 coastline. The event caused overtopping at East Beach in West Bay and at Chesil Beach.

522 The second event, on 1st February 2021, was entirely driven by the swell waves travelling through the
523 English Channel. A complex low travelled across the channel but did not generate any significant wind
524 speeds or wave heights. The event generated some of the highest energy period measurements on
525 record at the buoys deployed in the channel and caused waves to run up over the promenades in
526 Poole and Christchurch Bays and caused overtopping and flattening of the beach crest at Hayling
527 Island.

528 Spatial footprints of both events were generated through joint return period analysis of water level
529 combined with one wave parameter; significant wave height H_s , energy period T_e or wave power P .
530 The water level at which a swell event occurs will significantly contribute to the severity of the impact
531 of that event in terms of overtopping or beach erosion. T_e was calculated to provide a smoother time
532 series for swell monitoring than T_p . As the ratio of the first negative and zero moments of the wave
533 spectrum, the energy period represents more of the lower frequency energy in the spectrum whilst
534 avoiding marked jumps in the time series. Wave power P was calculated in an attempt to account for
535 both wave heights and wave period in a single parameter.

536 The 31st January swell event, with its significant contribution of moderate wave heights due to the low
537 centred off Land's end was best described by the joint return periods of water level and wave power.
538 The 1st February event is almost entirely driven by swell and therefore best captured by the joint return
539 periods of water level and T_e .

540 Finally, T_e was found to be a valuable addition to the standard wave parameters used to describe the
541 two swell events under discussion. T_e , providing a smoother time series than the rapidly changing T_p ,
542 allowed for improved quantification of the swell energy and has the potential for threshold setting for
543 'swell alerts.' The parameter could also prove useful in supporting modelling efforts, in particular
544 overtopping models, by providing a check on predictions. It is therefore recommended that T_e is
545 considered for inclusion in the arsenal of wave parameters currently used for coastal monitoring and
546 beach management purposes. Also wave power P , as a measure of both wave height and period, could
547 be a valuable addition for those events where swell is combined with a significant amount of wind-
548 generated waves, although in theory these could be monitored by observing both H_s and T_e . Inclusion
549 of these parameters will ensure that those swell events with the potential to impact coastal flooding
550 and erosion, but which aren't currently captured in standard flood warning models, can be more
551 closely monitored.

552 **Conflict of interest statement**

553 The authors declare that they have no conflict of interest.

554 **Acknowledgements**

555 The authors would like to thank Dr Sam Cope and Dr Andy Pearce from the Coastal Partners team at
556 Havant Borough Council, Dr Matthew Wadey from Bournemouth, Christchurch and Poole Council, Jack
557 Eade from Jacobs, and Martin Worley and Dave Picksley from the Environment Agency for the
558 information and images they provided. The authors also thank Robin Newman from Fugro for
559 providing valuable feedback on an early draft of this paper.

560 The National Network of Regional Coastal Monitoring Programmes (NNRCMP) is funded by the
561 Department for Environment, Food and Rural Affairs (DEFRA) through the Environment Agency. Data
562 is made available under Open Government License. The analysis also included data provided by CEFAS
563 which is also funded by DEFRA through the Environment Agency. Data is licensed under the Cefas
564 WaveNet Non-Commercial License v1.0. This study also uses data from the National Tidal and Sea
565 Level Facility, provided by the British Oceanographic Data Centre and funded by the Environment
566 Agency.

567 **Contributor's statement**

568 Thomas Dhoop conceptualised the study, performed the analysis and wrote the original draft of the
569 paper. Charlie Thompson provided supervision over the work, and reviewed and edited the original
570 draft.

571 **Funding statement**

572 The Channel Coastal Observatory, as part of the National Network of Regional Coastal Monitoring
573 Programmes (NNRCMP) is funded by the Department for Environment, Food and Rural Affairs (DEFRA)
574 through the Environment Agency.

575

576 **Data availability statement**

577 The wave data used in this study, provided by the NNRCMP is publicly available under open
578 government license from www.coastalmonitoring.org. The wave data provided by CEFAS is publicly
579 available under the Cefas WaveNet Non-commercial License v1.0 from www.wavenet.cefas.co.uk. The
580 tide data provided by the National Tide and Sea Level Facility is publicly available through the British
581 Oceanographic Data Centre (BODC) from www.ntsif.org.

582 **References**

- 583 Bernardara, P., Mazas, F., Kergadallan, X., and Hamm, L. 2014. A two-step framework for over-
584 threshold modelling of environmental extremes. *Nat. Hazards Earth Syst. Sci.* **14**: 635-647.
585 doi:10.5194/nhess-14-635-2014
- 586 Bradbury, A., Mason, T. and Poate, T. 2007. Implications of the spectral shape of wave conditions for
587 engineering design and coastal hazard assessment – Evidence from the English Channel. *In* 10th
588 International Workshop on Wave Hindcasting and Forecasting and Coastal Hazard Symposium.
589 <http://www.waveworkshop.org/10thWaves/ProgramFrameset.htm>
- 590 Bradbury, A., Stratton, M. and Mason, T. 2011. Impacts of wave climate with bi-modal wave period on
591 the profile response of gravel beaches. *In* The Proceedings of Coastal Sediments 2011. *Edited by* J.D.
592 Rosati, P. Wang and T.M. Roberts. World Scientific Publishing, Singapore, pp. 2004-2018.
593 doi.org/10.1142/9789814355537_0151
- 594 Carr, A. 1983. Chesil beach: environmental, economic and sociological pressures. *Geogr. J.* **149**: 53-62.
595 doi.org/10.2307/633342
- 596 CEFAS, 2021. <https://www.cefas.co.uk/data-and-publications/wavenet/> Access: 12 May 2021.
- 597 Coles, S.G. 2001. An Introduction to Statistical Modelling of Extreme Values. Springer, London, UK. 209
598 pp.
- 599 Datawell. 2020. Datawell Waverider Reference Manual. Datawell BV.
600 https://www.datawell.nl/Portals/0/Documents/Manuals/datawell_manual_dwr-mk3_dwr-g_wr-
601 [sg_2020-02-01.pdf](https://www.datawell.nl/Portals/0/Documents/Manuals/datawell_manual_dwr-mk3_dwr-g_wr-sg_2020-02-01.pdf)
- 602 De Waal, D. and Van Gelder, P. 2005. Modelling of extreme wave heights and periods through
603 copulas. *Extremes.* **8.4**: 345-356. Doi.org/10.1007/s10687-006-0006-y

604 Dhoop, T. and Thompson, C. 2018. Extreme Value Analysis for NNRCMP Coastal Wave Data. Channel
605 Coastal Observatory.
606 <https://coastalmonitoring.org/reports/index.php?link=&dla=download&id=1517&cat=266/Extreme>
607 [Value Analysis for CCO Coastal Wave%20Data TN03.pdf](#)

608 Draper, L. and Bownass, T. 1983. Wave devastation behind Chesil beach. *Weather*. **38**: 346-352.
609 doi.org/10.1002/j.1477-8696.1983.tb04822.x

610 EurOtop. 2018. Manual on wave overtopping of sea defences and related structures. An overtopping
611 manual largely based on European research, but for worldwide application. Van der Meer, J.W., Allsop,
612 N.W.H., Bruce, T., De Rouck, J., Kortenhaus, A., Pullen, T., Schüttrumpf, H., Troch, P. and Zanuttigh, B.,
613 www.overtopping-manual.com.

614 Folley, M. 2016. The wave energy resource. *In Handbook of Ocean Wave Energy. Edited by A. Pecher*
615 *and J. Kofoed. Springer, Cham, Switzerland. pp. 43-79. doi.org/10.1007/978-3-319-39889-1_3*

616 Hawkes, P.J. 1999. Mean overtopping rate in swell and bimodal seas. *Proc. Instn Civ. Engr Wat., Marit.*
617 *& Energy*. **136**: 235-238. doi.org/10.1680/iwtme.1999.31987

618 Hawkes, P.J., Gouldby, B.P., Tawn, J.A. and Owen, M.W. 2002. The joint probability of waves and water
619 levels in coastal engineering design. *J. Hydraul. Res.* **40**: 241-251.
620 doi.org/10.1080/00221680209499940

621 Li, F., van Gelder, P.H.A.J.M., Ranasinghe, R., Callaghan, D.P. and Jongejan, R.B. 2014. Probabilistic
622 modelling of extreme storms along the Dutch coast. *Coastal Engineering*. **86**: 1-13.
623 doi.org/10.1016/j.coastaleng.2013.12.009

624 Malagon Santos, V., Haigh, I. and Wahl, T. 2017. Spatial and temporal clustering analysis of extreme
625 wave events around the UK coastline. *J. Mar. Sci. Eng.* **5**.28. doi.org/10.3390/jmse5030028

626 Mason, T. and Dhoop, T. 2018. Occurrence of bimodal seas around the English coastline. Technical
627 Note TN02. National Network of Regional Coastal Monitoring Programmes of England.

628 https://coastalmonitoring.org/reports/index.php?link=&dla=download&id=1518&cat=266/Occurrence_of_Bimodal_Seas_around_the_English_Coastline_TN02.pdf

629

630 Mazas, F. and Hamm, L. 2017. An event-based approach for extreme joint probabilities of waves and

631 sea levels. *Coastal Engineering*. **122**: 44-59. doi.org/10.1016/j.coastaleng.2017.02.003

632 NNRCMP, 2021. <https://coastalmonitoring.org/> Access: 12 May 2021.

633 Palmer, R., Nicholls, R.J., Wells, N.C., Saulter, A., Mason, T. 2014. Identification of ‘energetic’ swell

634 waves in a tidal strait. *Continental Shelf Research*. **88**: 203-205. doi.org/10.1016/j.csr.2014.08.004

635 Poate, T.G., McCall, R.T. and Masselink, G. 2016. A new parameterisation for runup on gravel beaches.

636 *Coastal Engineering*. **117**: 176-190. doi.org/10.1016/j.coastaleng.2016.08.003

637 Serinaldi, F. 2015. Dismissing return periods. *Stoch. Environ. Res. Risk Assess.* **29**: 1179-1189.

638 doi.org/10.1007/s00477-014-0916-1

639 Sibley, A. and Cox, D. 2014. Flooding along the English Channel coast due to long-period swell waves.

640 *Weather* **69**: 59-66. doi.org/10.1002/wea.2145

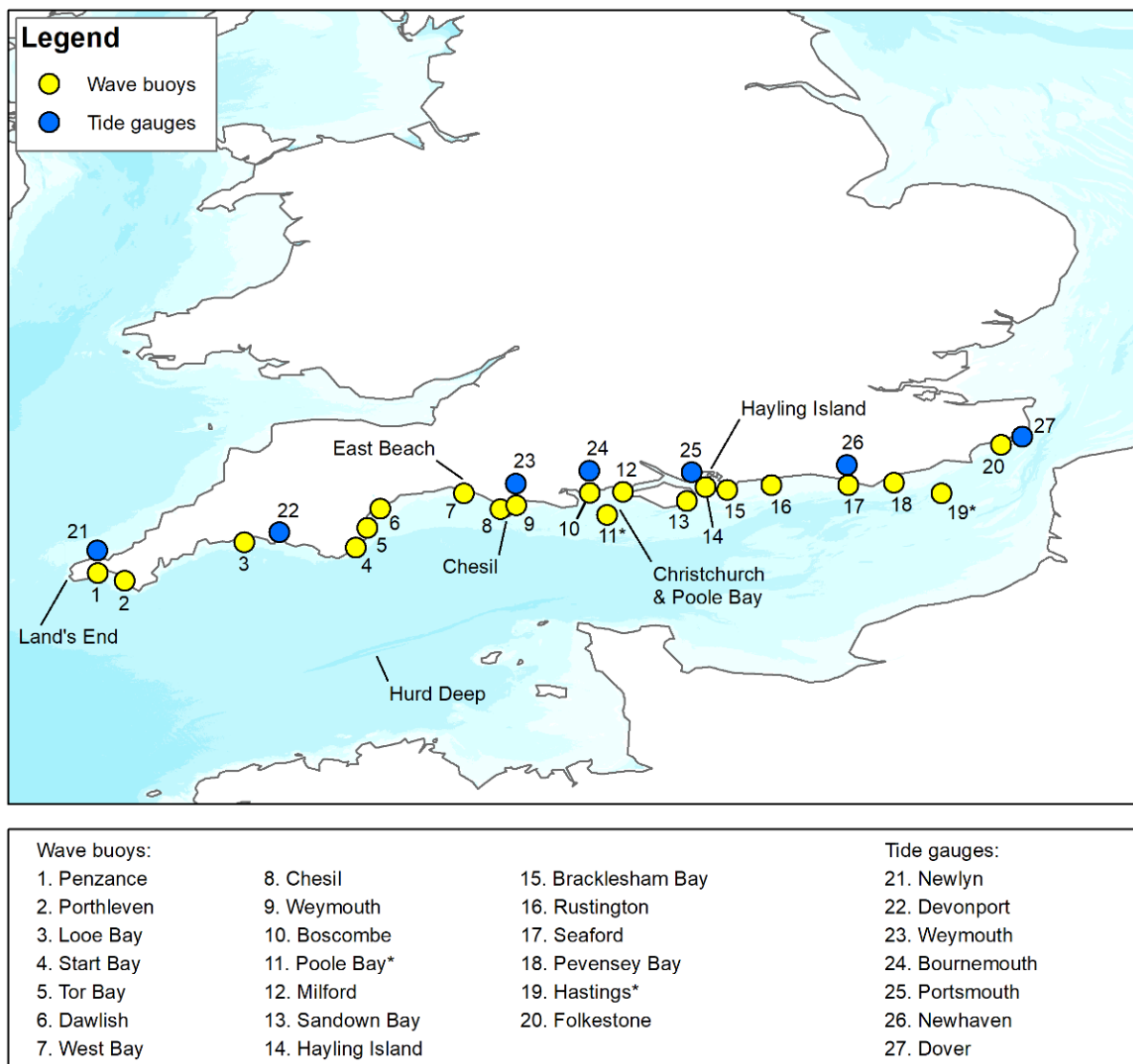
641 Sklar, A. 1959. Fonctions de repartition à n dimensions et leurs marges. *Publications de l’Institut*

642 *Statistique de L’Université de Paris*. **8**: 229-230.

643 Wahl, T., Muddersbach, C. and Jensen, J. 2012. Assessing the hydrodynamic boundary conditions for

644 risk analyses in coastal areas: a multivariate statistical approach based on copula functions. *Nat.*

645 *Hazards Earth Syst. Sci.* **12**: 495-510.



647

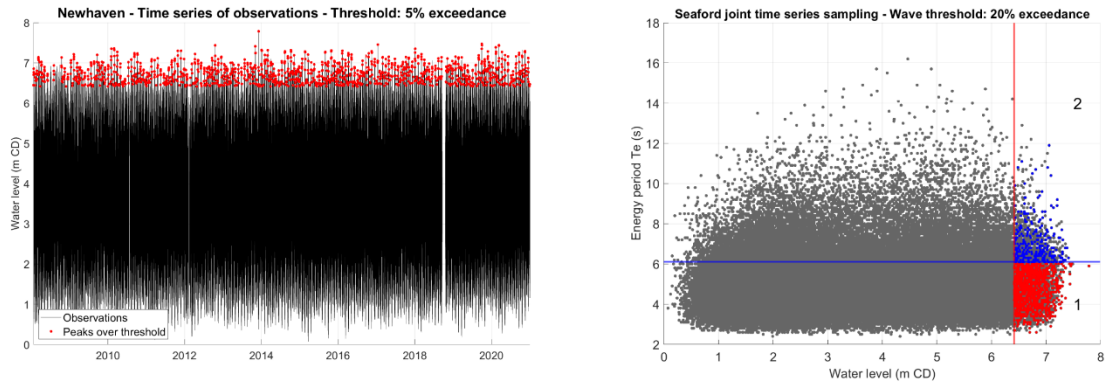
648 Figure 1: Locations of the wave buoys and tide gauges used in this study. All wave buoys are owned and operated
 649 by the NNRCMP, except those indicated with an asterisk which are owned and operated by CEFAS. All tide gauges
 650 are owned and operated by the UK National Tide Gauge Network.

651

652

653

654

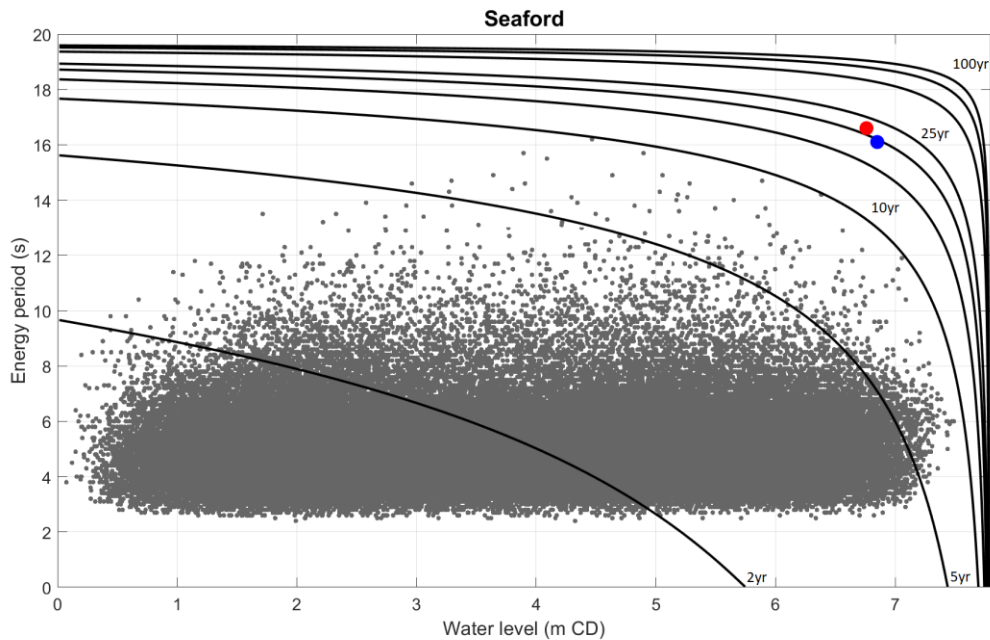


655

656 Figure 2: Sample of high water levels extracted via peaks over threshold from the concurrent sample of water
 657 levels at Newhaven and waves from the Seaford DWR (left).

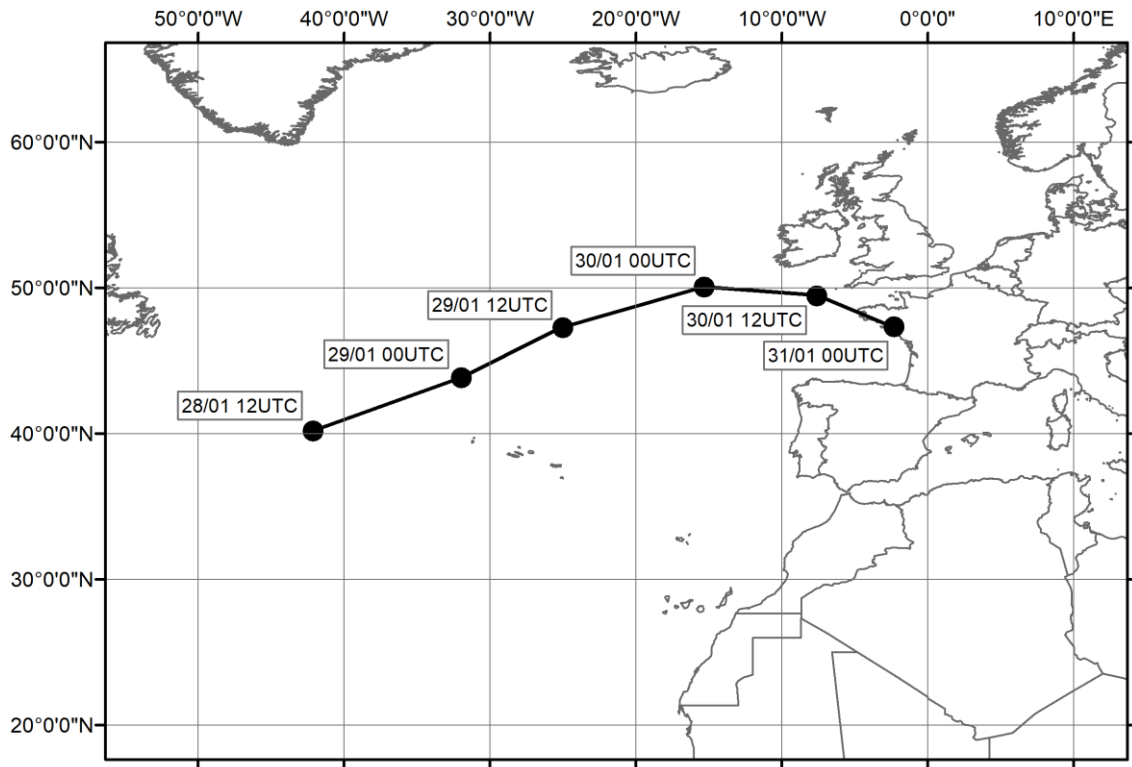
658 From the sample of high water levels from Newhaven (quadrants 1 + 2), a subsample is extracted for dependence
 659 modelling by applying a high threshold for energy period T_e from the Seaford DWR (blue line, 20% exceedance
 660 in this example), resulting in the sample represented by the blue markers in quadrant 2 (right).

661



662

663 Figure 3: Joint return period plot of water level and energy period T_e . In red, peak T_e is indicated with the
 664 associated water level. In blue, the highest water level during the event is indicated with the associated T_e . The
 665 values are from the 1st February 2021 swell event.



666

667

Figure 4: Storm track of the 30th January 2021 swell event.

668

Date / Time (UTC)	Barometric Pressure (mb)	Latitude / Longitude	Km	Km/h / knots
28/01 12:00	973	40°N, 40°W	-	-
29/01 00:00	967	44°N, 32°W	798	67 / 36
29/01 12:00	968	47°N, 25°W	629	52 / 28
30/01 00:00	975	50°N, 15°W	811	68 / 36
30/01 12:00	981	50°N, 08°W	498	42 / 22
31/01 00:00	993	48°N, 03°W	427	36 / 19

669 Table 1: Time, central pressure, position, distance travelled and estimated average speed of movement of the

670 depression for the 30th January 2021 event.

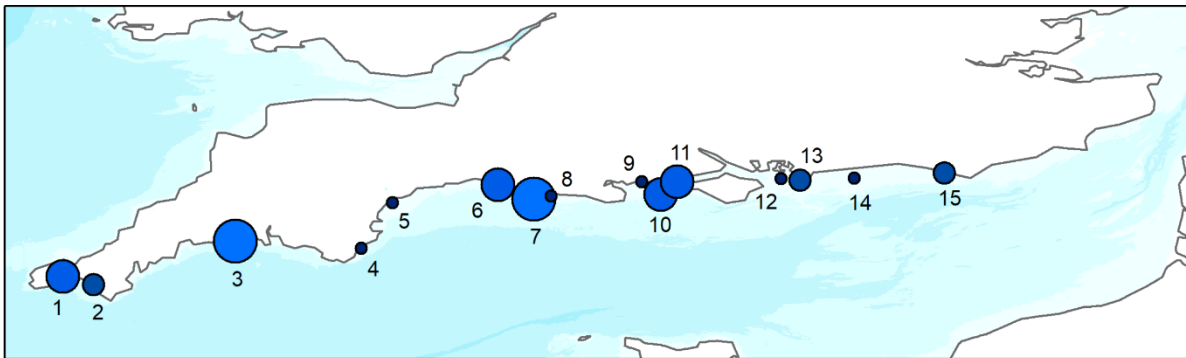
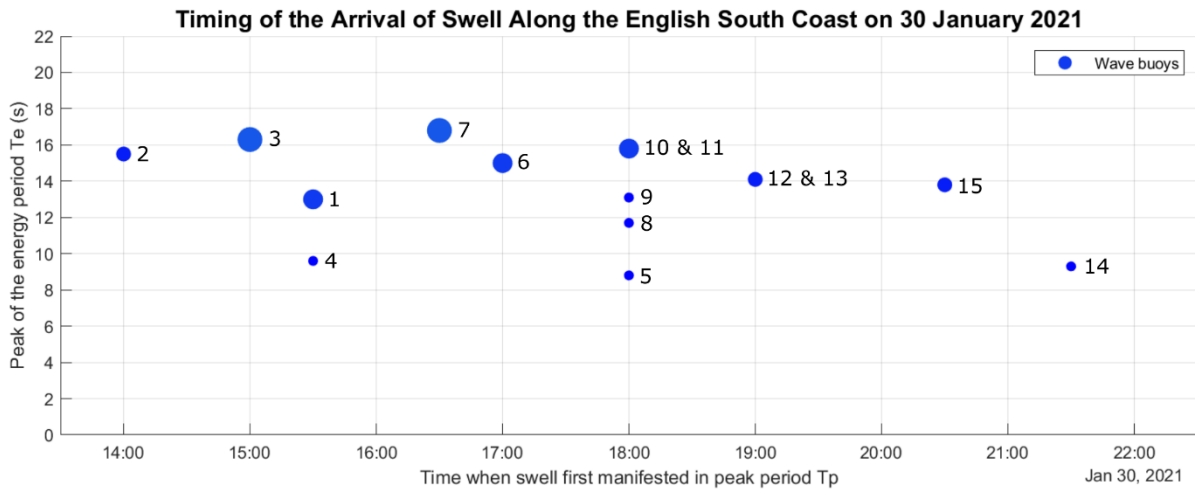
671

672

673

674

675



Site	Return Period	Site	Return Period	Legend
1. Penzance	1 year	9. Boscombe	Bel. thr.	
2. Porthleven	0.25 year	10. Poole Bay	1 year	● 0.25 year
3. Looe Bay	2 year	11. Milford	1 year	● 1 year
4. Start Bay	Bel. thr.	12. Hayling Island	Bel. thr.	● 2 year
5. Dawlish	Bel. thr.	13. Bracklesham Bay	0.25 year	
6. West Bay	1 year	14. Rustington	Bel. thr.	
7. Chesil	2 year	15. Seaford	0.25 year	
8. Weymouth	Bel. thr.			

676

677 Figure 5: The swell propagating through the English Channel on 30th January 2021. The x-axis denotes when swell

678 first manifested in peak period T_p , the y-axis shows the peak energy period T_e achieved during the event. The

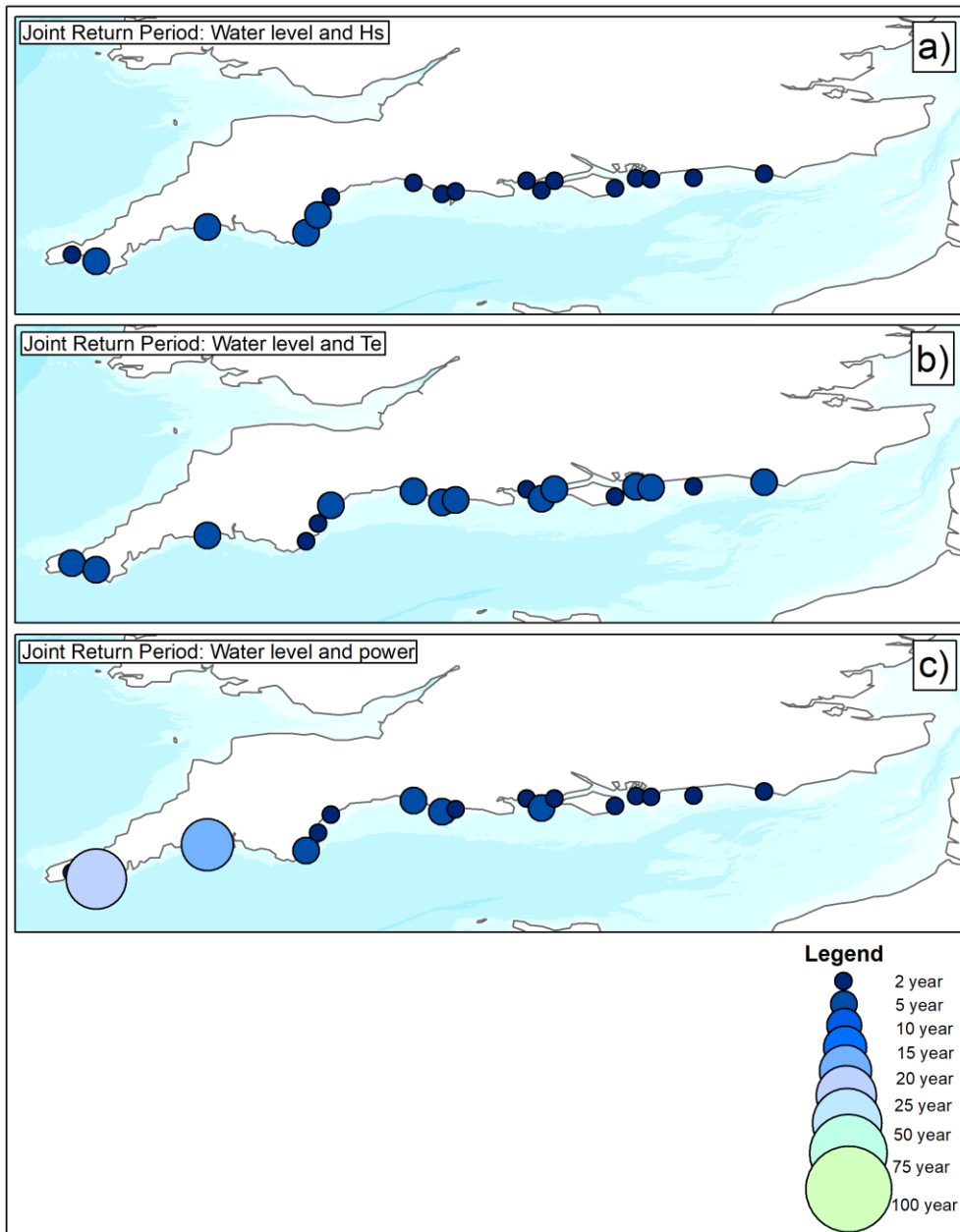
679 size of the markers gives an indication of the T_e return period achieved at the site. On the map, the size of the

680 marker is relative to the T_e return period achieved at each wave buoy site.

681

682

683



684

685 Figure 6: Spatial footprints of the 30th January 2021 swell event. The size of the markers is congruent with the
 686 joint return period achieved at the site. The spatial extent of the swell events is shown by mapping the joint
 687 return periods of water level and one of three wave parameters: significant wave height Hs (a), energy period
 688 Te (b) and wave power P (c).

689

690



691

692

Figure 7: Beach erosion at East Beach, West Bay on 1st February 2021. Photo by the Environment Agency.

693

694

695

696

697

698

699

700

701

Date: 30/01/2021 Time: 11:41 Citizen Scientist: Jane Id: 286

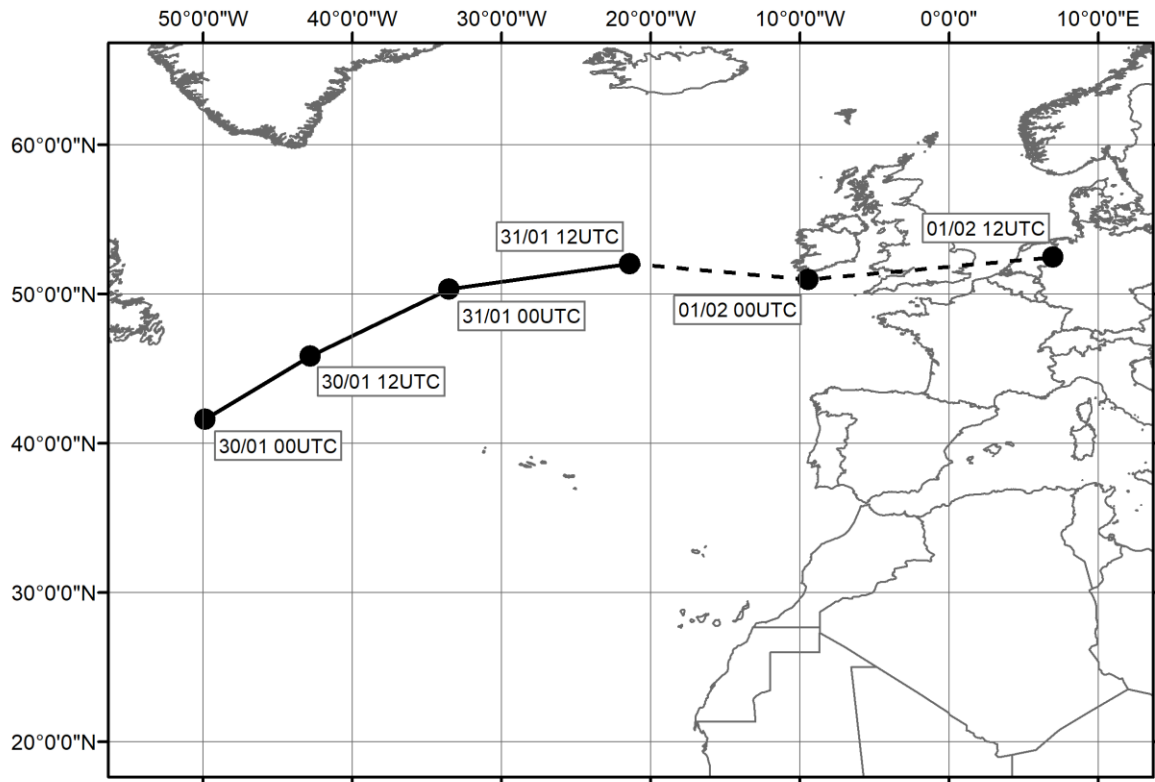


Date: 31/01/2021 Time: 16:02 Citizen Scientist: NA Id: 296



702

703 Figure 8: Erosion at Chesil Beach. The top photo was taken on 30th January, the bottom photo on 31st January
704 2021. Photo by the Southwest Regional Coastal Monitoring Programme CoastSnap Project.



705

706 Figure 9: Storm track of the 1st February 2021 swell event. The hashed line is the track once the depression had
 707 lost its identity and became a complex low.

708

Date / Time (UTC)	Barometric Pressure (mb)	Latitude / Longitude	Km	Km/h / knots
30/01 00:00	957	42°N, 50°W	-	-
30/01 12:00	962	46°N, 43°W	740	62 / 33
31/01 00:00	969	50°N, 34°W	854	71 / 38
31/01 12:00	978	52°N, 21°W	863	72 / 39
01/02 00:00	987	51°N, 10°W	842	70 / 38
01/02 12:00	993	52°N, 07°E	-	-

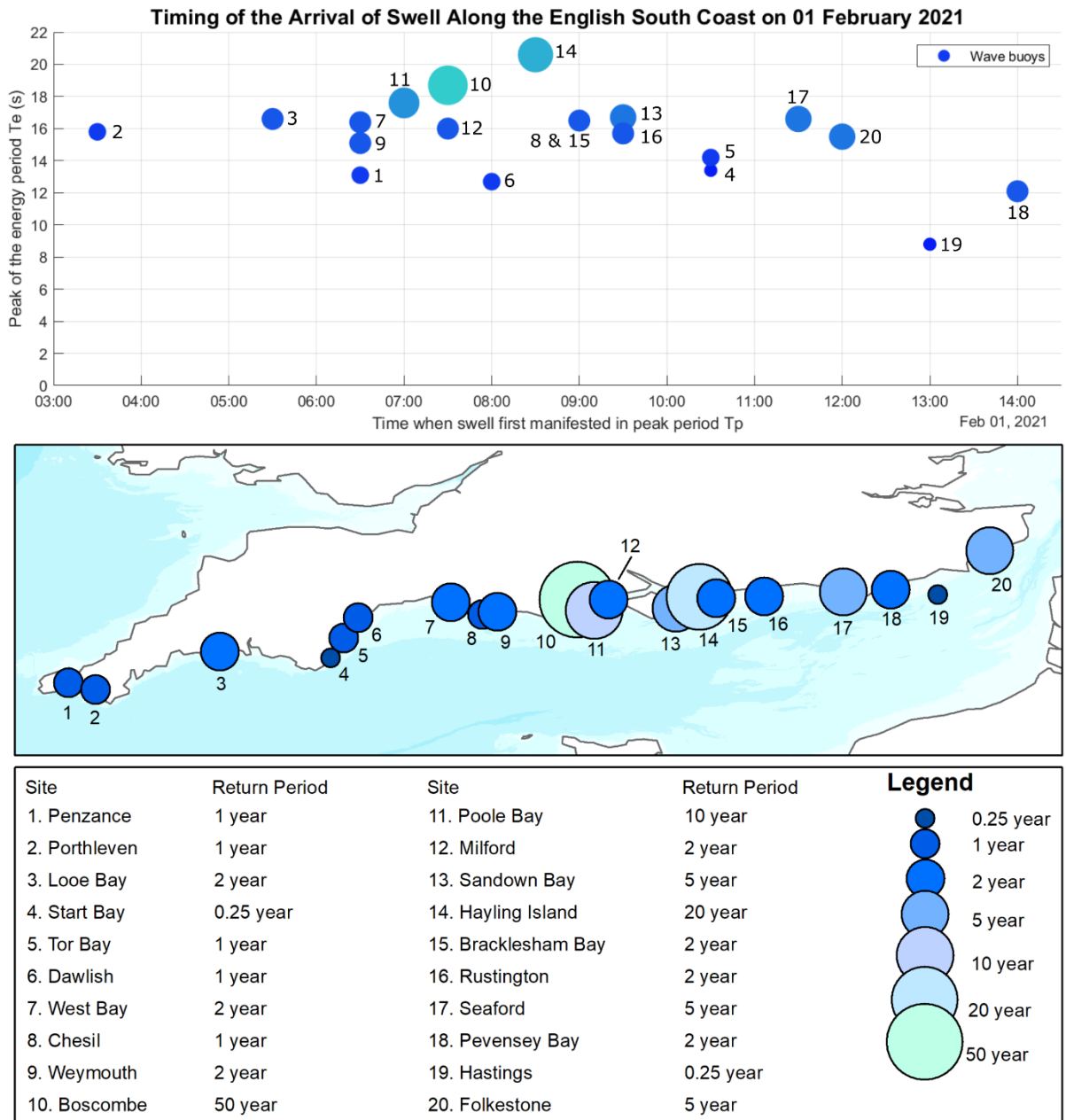
709 Table 2: Time, central pressure, position, distance travelled and estimated average speed of movement of the
 710 depression for the 1st February 2021 event.

711

712

713

714

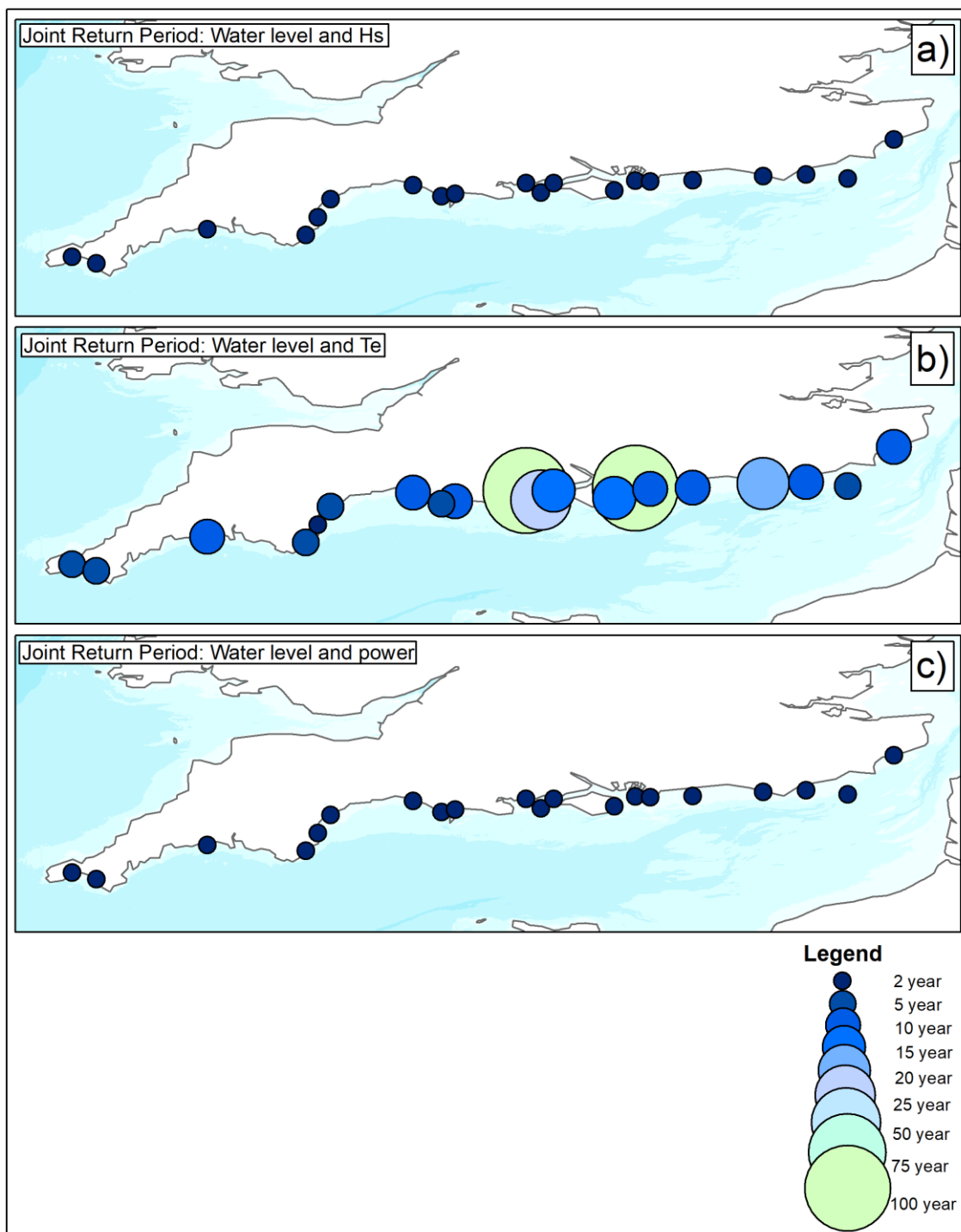


716

717 Figure 10: The swell propagating through the English Channel on 1st February 2021. The x-axis denotes when
 718 swell first manifested in peak period T_p , the y-axis shows the peak energy period T_e achieved during the event.
 719 The size of the markers give an indication of the T_e return period achieved at the site. On the map, the size of
 720 the marker is relative to the T_e return period achieved at each wave buoy site.

721

722



724

725 Figure 11: Spatial footprints of the 1st February 2021 swell event. The size of the markers is congruent with the
 726 joint return period achieved at the site. The spatial extent of the swell events is shown by mapping the joint
 727 return periods of water level and one of three wave parameters: significant wave height Hs (a), energy period
 728 Te (b) and wave power P (c).

729



730

731

Figure 12: Overtopping at Hayling Island on 1st February 2021. Photo by Havant Borough Council.

732



733

734 Figure 13: Plant is deployed at Hayling Island for emergency repairs to the beach. Photo by Havant Borough
735 Council.

736

737

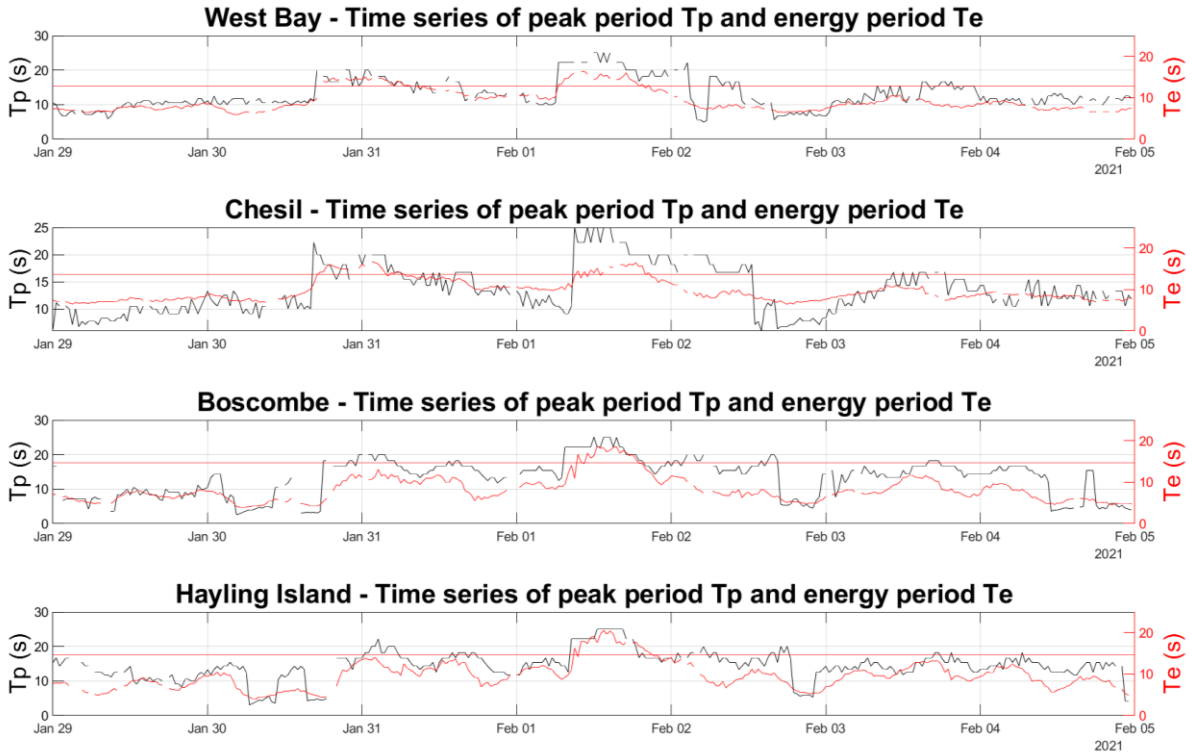
738

739

740

741

742



743

744 Figure 14: Time series of peak period T_p (black) and energy period T_e (red) at those sites with reported impacts
 745 from the 30th January and 1st February swell events. The red horizontal line represents the 0.25 year return
 746 period for energy period T_e as an indicative swell alert threshold.

747 **Appendix 1**

748 The wave energy period T_e can be defined as the ratio of the first negative moment of the spectrum
749 to the zeroth moment as given by equation A1.

750
$$T_e = \frac{m_{-1}}{m_0} \quad [A1]$$

751 When knowledge of the full wave spectrum is not available, the energy period T_e can still be derived
752 from the full spectral parameter output of a Datawell MkIII buoy, specifically the periods T_{dw2} and
753 T_1 . What Datawell refers to as T_{dw2} is the wave period $T_m(-1,1)$ and is defined as the square root of
754 the ratio of the first negative moment of the spectrum to the first moment as given by equation A2.

755
$$T_{dw2} = \sqrt{\frac{m_{-1}}{m_1}} \quad [A2]$$

756 What Datawell refers to as T_1 is the mean wave period or $T_m(0,1)$ and is defined as the ratio of the
757 zeroth moment of the spectrum to the first moment as given by equation A3.

758
$$T_1 = \frac{m_0}{m_1} \quad [A3]$$

759 The wave energy period T_e can therefore be calculated from the standard spectral analysis output of
760 a Datawell Directional Waverider MkIII by reformulating equation A1 as:

761
$$T_e = \frac{m_{-1}}{m_0} = \frac{T_{dw2}^2}{T_1} \quad [A4]$$